Molecular Therapy
Original Article

IMPDH1/YB-1 Positive Feedback Loop Assembles Cytoophidia and Represents a Therapeutic Target in Metastatic Tumors

Hailong Ruan,[1,2,5] Zhengshuai Song,[1,2,5] Qi Cao,[1,2,5] Dong Ni,[1,2] Tianbo Xu,[1,2] Keshan Wang,[1,2] Lin Bao,[1,2] Junwei Tong,[1,2] Haibing Xiao,[1,2] Wen Xiao,[1,2] Gong Cheng,[1,2] Zhiyong Xiong,[1,2] Huageng Liang,[1,2] Di Liu,[1,2] Liang Wang,[1,2] Tredan Olivier,[3] Boyle Helen Jane,[3] Hongmei Yang,[4] Xiaoping Zhang,[1,2] and Ke Chen[1,2]

[1]Department of Urology, Union Hospital, Tongji Medical College, Huazhong University of Science and Technology, Wuhan 430022, China; [2]Institute of Urology, Union Hospital, Tongji Medical College, Huazhong University of Science and Technology, Wuhan 430022, China; [3]Department of Oncology, Centre Leon Berard, 28 Prom. Léa et Napoléon Bullukian, 69008 Lyon, France; [4]Department of Pathogenic Biology, School of Basic Medicine, Huazhong University of Science and Technology, Wuhan 430030, China

Recently, cytoophidium, a nonmembrane-bound intracellular polymeric structure, has been shown to exist in various organisms, including tumor tissues, but its function and mechanism have not yet been examined. Examination of cytoophidia-assembled gene inosine monophosphate dehydrogenase (IMPDH) and cytidine triphosphate synthetase (CTPS) mRNA levels showed that only IMPDH1 levels were significantly higher in the clear cell renal cell carcinoma (ccRCC). IMPDH1 was positively correlated with the metastasis-related gene Y-box binding protein 1 (YB-1) and served as an independent prognostic factor in ccRCC. Kaplan-Meier analysis indicated that patients with tumors that expressed high IMPDH1 levels had a shorter overall survival (OS) and disease-free survival (DFS). Furthermore, detection of cytoophidia by immunofluorescence staining in ccRCC tissues showed that IMPDH1-assembled cytoophidia are positively associated with tumor metastasis. Mechanistically, IMPDH1 and YB-1 formed an autoregulatory positive feedback loop: IMPDH1 maintained YB-1 protein stabilization; YB-1 induced IMPDH1 expression by binding to the IMPDH1 promoter motif. Functionally, IMPDH1-assembled cytoophidia physically interacted with YB-1 and translocated YB-1 into the cell nucleus, thus correlating with ccRCC metastasis. Our findings provide the first solid theoretical rationale for targeting the IMPDH1/YB-1 axis to improve metastatic renal cancer treatment.

INTRODUCTION

Renal cell carcinoma (RCC), which accounts for 80%–90% of renal malignancies and 2%–3% of adult malignancies, is mainly composed of clear cell renal cell carcinoma (ccRCC).[1] Techniques to understand ccRCC tumorigenesis and progression are centered on the concept that ccRCC is a metastatic and metabolic disease, whereby ccRCC cells are inclined toward specific gene mutations that empower metastatic and metabolic-related phenotypes. Cancer metastasis is predicted to account for more than 90% of tumor-related deaths.[2] The ccRCC, which is surrounded by extensive vascularization, possesses a special advantage for local invasion and distant metastasis.[3] Notwithstanding the progress in the understanding of the mechanisms involved in metastatic progression, the specific molecular mechanisms of ccRCC metastasis remain unclear. Despite aggressive surgical treatment, molecular-targeted therapy, and multidisciplinary treatment, prognosis of metastatic and advanced ccRCC remains formidable.

In 2010, three independent study groups[4–6] found that cytidine triphosphate synthetase (CTPS), a rate-limiting enzyme in the *de novo* synthesis of nucleotide cytidine triphosphate (CTP), can assemble filamentous structures named cytoophidia (Greek, meaning cellular snakes). This structure is not membrane bound and not associated with any known organelle in mammalian cells. Inosine monophosphate dehydrogenase (IMPDH), a rate-limiting enzyme of guanosine triphosphate (GTP) *de novo* synthesis,[7] can also form a filamentous structure similar to the CTPS-assembled cytoophidia.[8] IMPDH has two diffusely expressed isozymes: IMPDH1 and IMPDH2.[9] As a pivotal regulator of the intracellular GTP pool, IMPDH is required for DNA and RNA synthesis and for signal transduction in almost all organisms.[10] The morphological structure of cytoophidia includes "rods and rings," "long and linear," and "spicule or dot" in human cells. However, in tumor tissues, the morphological structure of cytoophidia is mainly dot like or filamentous depending on the tumor tissue type.[10,11] The cytoophidia might be associated

Received 23 September 2019; accepted 5 March 2020;
https://doi.org/10.1016/j.ymthe.2020.03.001.

[5]These authors contributed equally to this work.

Correspondence: Ke Chen, Department of Urology, Union Hospital, Tongji Medical College, Huazhong University of Science and Technology, 1277 Jiefang Avenue, Wuhan 430022, Hubei Province, China.
E-mail: shenke@hust.edu.cn
Correspondence: Xiaoping Zhang, Department of Urology, Union Hospital, Tongji Medical College, Huazhong University of Science and Technology, 1277 Jiefang Avenue, Wuhan 430022, Hubei Province, China.
E-mail: xzhang@hust.edu.cn

with the tumor cell proliferation rate and metabolic preference and limited blood supply in hepatocellular carcinoma.[11] A recent study[11] has shown that cytoophidia exist in various tumor tissues, but their function and mechanism in renal cancer therein remain unclear.

Y-box binding protein 1 (YB-1), which belongs to the cold-shock domain (CSD) protein family, has been highly conserved during evolution.[12] Eukaryotic YB-1 proteins are implicated in a wide range of cellular biological functions, such as orchestrating transcription, as well as RNA translation by binding DNA or RNA[13,14] and playing proto-oncogenic roles in epithelial-mesenchymal transformation (EMT), cell migration, and drug resistance in various malignancies.[15–19] In particular, YB-1 increases the transcription of cyclin A, topoisomerase IIa, and androgen receptor (AR).[20–22] Translationally, YB-1 activates Snail1 and other developmentally regulated transcription factors to promote epithelial-mesenchymal transformation.[15] It also activates hypoxia-inducible factor-1α (HIF1α) to promote sarcoma metastasis.[16] Regarding the expression levels of YB-1 in tumors, YB-1 was reported to be upregulated in breast cancer and associated with a drug-resistance phenotype.[23] As for other malignant tumors, YB-1 was also reported to be overexpressed in prostate cancer, colorectal carcinoma, medulloblastoma, pancreatic adenocarcinoma, and ovarian carcinoma.[24] Additionally, a recent study demonstrated that YB-1 overexpression promotes RCC cell invasion.[25] However, how YB-1 enters the nucleus to promote the metastasis of kidney cancer remains unclear.

In this study, for the first time, we found that IMPDH1-assembled cytoophidia translocated YB-1 into the cell nucleus and correlated with tumor metastasis. IMPDH1 and YB-1 formed an autoregulatory positive feedback loop. Our findings reveal the function and mechanisms of IMPDH1 in tumors. The IMPDH1/YB-1 positive feedback loop may serve as therapeutic targets in metastatic RCC (mRCC) and advanced RCC.

RESULTS

IMPDH1-Assembled Cytoophidia Are Positively Associated with Tumor Metastasis

IMPDH and CTPS are the major metabolic enzymes that assemble the cytoophidia in mammalian cells, both of which have two isozymes, termed IMPDH1 and IMPDH2 and CTPS1 and CTPS2, respectively.[26] Although cytoophidia exist in various tumor tissues, the mechanisms and function of cytoophidia in renal tumors have not yet been examined. We first performed *in silico* analyses of IMPDH and CTPS expression using The Cancer Genome Atlas (TCGA) dataset composed of 534 ccRCC cases, including 72 paired cases. As shown in Figures 1A and S1A–S1C, only IMPDH1 mRNA levels were significantly higher in the ccRCC tissues than in the normal tissues, and the patients with metastasis had a higher IMPDH1 expression than the patients with no metastasis. Furthermore, a Kaplan-Meier analysis was conducted to determine whether the overall survival (OS) and disease-free survival (DFS) of patients were associated with IMPDH and CTPS expression in tumors. The Kaplan-Meier analysis indicated that patients with tumors that only expressed high IMPDH1 levels had a shorter OS and DFS (Figure 1A; Figures S1A–S1C). Then, receiver operating characteristic (ROC) curves were used to analyze the diagnostic value of IMPDH1 for ccRCC in 72 paired cases from the ccRCC TCGA database. As shown in Figure 1B, IMPDH1 had a high area under the curve (AUC) in ccRCC patients, which means that IMPDH1 could effectively distinguish ccRCC patients from normal tissues. Next, according to the deep analysis of TCGA database, we found that high IMPDH1 expression was positively correlated with tumor stage and grade (Figure 1C; Table 1) and served as an independent prognostic factor (Table 2). To confirm the analysis in TCGA database, we performed *in silico* analyses of IMPDH1 expression using the Oncomine database. Similar to our previous results, IMPDH1 mRNA levels were significantly higher in ccRCC than in normal tissues (Figure 1D).

A recent study reported that cytoophidia are naturally present in a variety of tumor tissues, including renal cancer tissues.[11] After confirming the upregulation of the cytoophidia-assembled protein IMPDH1 in ccRCC and metastatic ccRCC tissues, we performed immunofluorescence staining analysis in adjacent normal tissues, ccRCC tissues, and metastatic ccRCC tissues. As shown in Figures 1E, S1D, and S1E, the number of IMPDH1-assembled cytoophidia increased in ccRCC and metastatic ccRCC. Additionally, the number of IMPDH1-assembled cytoophidia and the ratio of IMPDH1-assembled cytoophidia in the nucleus were also highest in metastatic ccRCC (Figures 1E, S1D, and S1E). The above results indicate that IMPDH1-assembled cytoophidia are positively associated with ccRCC metastasis.

IMPDH1 Expression Positively Correlates with EMT Markers and YB-1 Expression

To further identify the relationship between IMPDH1 and the tumor metastasis signaling pathways, we performed gene set enrichment analysis (GSEA) to analyze the gene sets that were altered by IMPDH1 expression in the ccRCC TCGA dataset. Our results showed that the metastasis, EMT, and hypoxia signaling pathways were highly associated with IMPDH1 expression (Figure 2A), suggesting that IMPDH1 is involved in the regulation of tumor metastasis in ccRCC. Previous studies have shown that YB-1 activates Snail1 and other developmentally regulated transcription factors to promote EMT[15] and activates HIF1α to promote tumor metastasis.[16] Then, we analyzed the correlation between IMPDH1 and EMT markers. As shown in Figure 2B, IMPDH1 was positively correlated with YB-1 and mesenchymal markers, including snail, slug, vimentin, and TWIST1, whereas a negative correlation was identified between IMPDH1 and epithelial markers, including E-cadherin and Krüppel-like factor 4 (KLF4).

Next, we assessed the clinical significance of YB-1 in the ccRCC TCGA database and found that the results were all consistent with IMPDH1. As shown in Figure 2C, YB-1 mRNA levels were significantly higher in the ccRCC tissues than in the normal tissues. Moreover, in metastatic ccRCC tissues, YB-1 expression levels were higher compared to no metastatic ccRCC tissues. Kaplan-Meier analysis indicated that patients with tumors that expressed high YB-1 levels had a shorter OS ($p = 0.0016$) and DFS ($p = 0.0002$) (Figure 2C). The GSEA analysis also

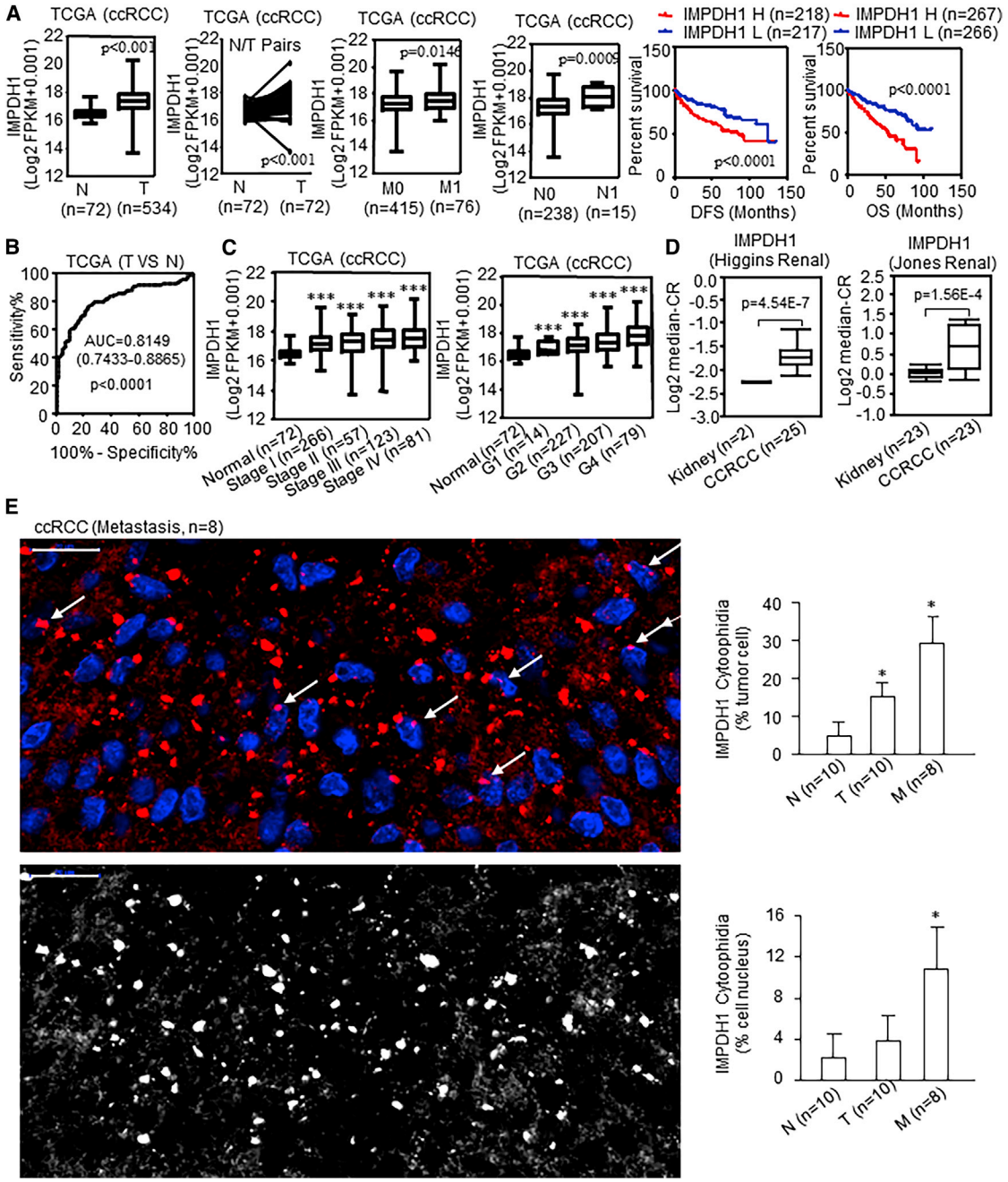

Figure 1. IMPDH1-Assembled Cytoophidia Are Positively Associated with Tumor Metastasis

(A) IMPDH1 mRNA levels were significantly elevated in TCGA dataset composed of 534 ccRCC cases, including 72 paired cases (N, normal tissues; T, tumor tissues; M0, M0 stage; M1, M1 stage; N0, N0 stage; N1, N1 stage). Kaplan-Meier analysis of IMPDH1 in ccRCC patients for OS and DFS. (B) Receiver operating characteristic (ROC) curves were used to analyze the diagnostic value of IMPDH1 for ccRCC in 72 paired cases from the ccRCC TCGA database. (C) High IMPDH1 expression was positively correlated with tumor stage and grade (G, grade). (D) IMPDH1 was upregulated in ccRCC tissues compared with normal tissues in Higgins and Jones studies. (E) Immunofluorescence staining analysis was performed to evaluate IMPDH1-assembled cytoophidia in metastatic ccRCC tissues (N, normal tissues; T, tumor tissues; M, metastatic tissues; scale bars, 20 μm). White arrows are referred to as IMPDH1 cytoophidia presented in the nucleus. The immunostaining quantification methods were to count the number of cytoophidia entering into the nucleus in each field of view and then take the average of three fields of view. The presentation of the histogram was the result of three independent experiments. ***$p < 0.001$, *$p < 0.05$, compared with the normal tissues.

Table 1. Correlation between IMPDH1 mRNA Expression and Clinicopathological Parameters of ccRCC Patients

			IMPDH1 mRNA Expression		
Parameter		Number	Low (n = 262)	High (n = 261)	p Value
Age (years)	≤60	260	130	130	
	>60	263	132	131	0.965
Gender	male	341	152	189	
	female	182	110	72	0.001
T stage	T1 + T2	334	183	151	
	T3 + T4	189	79	110	0.004
N stage	N0 + NX	507	259	248	
	N1	16	3	13	0.011
M stage	M0 + MX	446	233	213	
	M1	77	29	48	0.018
G stage	G1 + G2 + GX	244	147	97	
	G3 + G4	279	115	164	0.000
TNM stage	I + II	316	177	139	
	III + IV	207	85	122	0.001
Laterality	left	246	110	136	
	right	277	152	125	0.020

TNM, tumor, lymph node, metastasis.

Table 2. Cox Regression Analysis of Prognostic Risk Factors and Patient Overall Survival

	Univariate Analysis			Multivariate Analysis		
Risk Factors	HR	95% CI	p Value	HR	95% CI	p Value
Gender	1.065	0.782–1.449	0.690			
Age	1.747	1.286–2.373	0.000	1.684	1.235–2.295	0.001
T stage	3.099	2.289–4.194	0.000	0.883	0.486–1.606	0.684
N stage	3.841	2.079–7.095	0.000	1.674	0.887–3.161	0.112
M stage	3.405	2.601–4.457	0.000	2.029	1.441–2.856	0.000
G stage	2.611	1.863–3.658	0.000	1.494	1.038–2.152	0.031
TNM stage	3.788	2.763–5.194	0.000	2.387	1.219–4.674	0.011
Laterality	0.714	0.529–0.962	0.027	0.760	0.561–1.030	0.077
IMPDH1 expression	2.448	1.784–3.359	0.000	2.111	1.522–2.928	0.000

HR, hazard ratio; CI, confidence interval.

showed that the metastasis, EMT, and hypoxia signaling pathways were highly associated with YB-1 expression (Figure S2A).

To further confirm the interaction between IMPDH1 and YB-1, we examined IMPDH1 and YB-1 protein levels by immunohistochemical (IHC) staining and western blot analysis in ccRCC cells and specimens. Similar to our previous result, we observed that IMPDH1 positively correlated with YB-1 expression (Figure 2D). Furthermore, IMPDH1 and YB-1 protein levels were both significantly higher in ccRCC than in normal tissues (Figures 2D, S2B, and S2C). As shown in Figure S2B, the expression of IMPDH2, a homologous protein of IMPDH1, was not elevated in renal cancer cells. The Kaplan-Meier analysis indicated that patients with tumors that expressed high IMPDH1 or YB-1 levels had a shorter OS (Figure 2D). IHC staining showed that the expression levels of IMPDH1 and YB-1, as well as the ratio of IMPDH1 and YB-1 in the nucleus, were higher in metastatic ccRCC (Figure S2D). Additionally, the expression levels of IMPDH1 were positively correlated with YB-1 in metastatic ccRCC tissues (Figure S2E). Taken together, these findings suggested that IMPDH1 was positively correlated with the expression of YB-1 and EMT markers in ccRCC.

IMPDH1 Positively Regulates Tumor Metastasis Signaling Pathways

As the positive correlation between IMPDH1 and metastasis, EMT signaling pathways raised the possibility that IMPDH1 may function through these pathways. To test this hypothesis, we performed mRNA sequencing in 786-O cells with stably knocked down IMPDH1. In addition, there was no significant change in the expression of IMPDH2 in renal cancer cells that stably knocked down IMPDH1, indicating that small hairpin (sh)IMPDH1 could not target IMPDH2 (Figure S3B). Sequencing results revealed that IMPDH1 knockdown in 786-O cells resulted in an increase in epithelial markers and a decrease in mesenchymal markers (Figure 3A). However, the sequencing results showed that IMPDH1 knockdown did not reduce YB-1 mRNA levels. Subsequently, Gene Ontology (GO) analysis showed that IMPDH1 knockdown could positively regulate the process of MET (mesenchymal-epithelial transformation) (Figure 3B). Kyoto Encyclopedia of Genes and Genomes (KEGG) enrichment analysis showed that the downregulated genes in IMPDH1 knockdown cells are mainly enriched in transcriptional misregulation in cancers, pathways in cancer, cell adhesion molecules (CAMs), and the Ras signaling pathway (Figure 3C), whereas the upregulated gene-enriched pathways include the tumor necrosis factor (TNF) signaling pathway (Figure S3A). Moreover, we verified the sequencing results at the protein level. As shown in Figure 3D, IMPDH1 knockdown increased E-cadherin levels and reduced the levels of N-cadherin, slug, and vimentin. However, IMPDH2 knockdown did not change the expression of EMT markers (Figure S3C). Taken together, these findings suggested that IMPDH1 could positively regulate tumor metastasis via EMT signaling pathways.

IMPDH1 and YB-1 Regulate Each Other and Form a Positive Feedback Loop

The positive correlation between IMPDH1 and YB-1 expression raised the possibility that IMPDH1 may function through interactions with YB-1. To test this hypothesis, we performed western blot analysis using 786-O and ACHN cells. As shown in Figure 4A, YB-1 protein

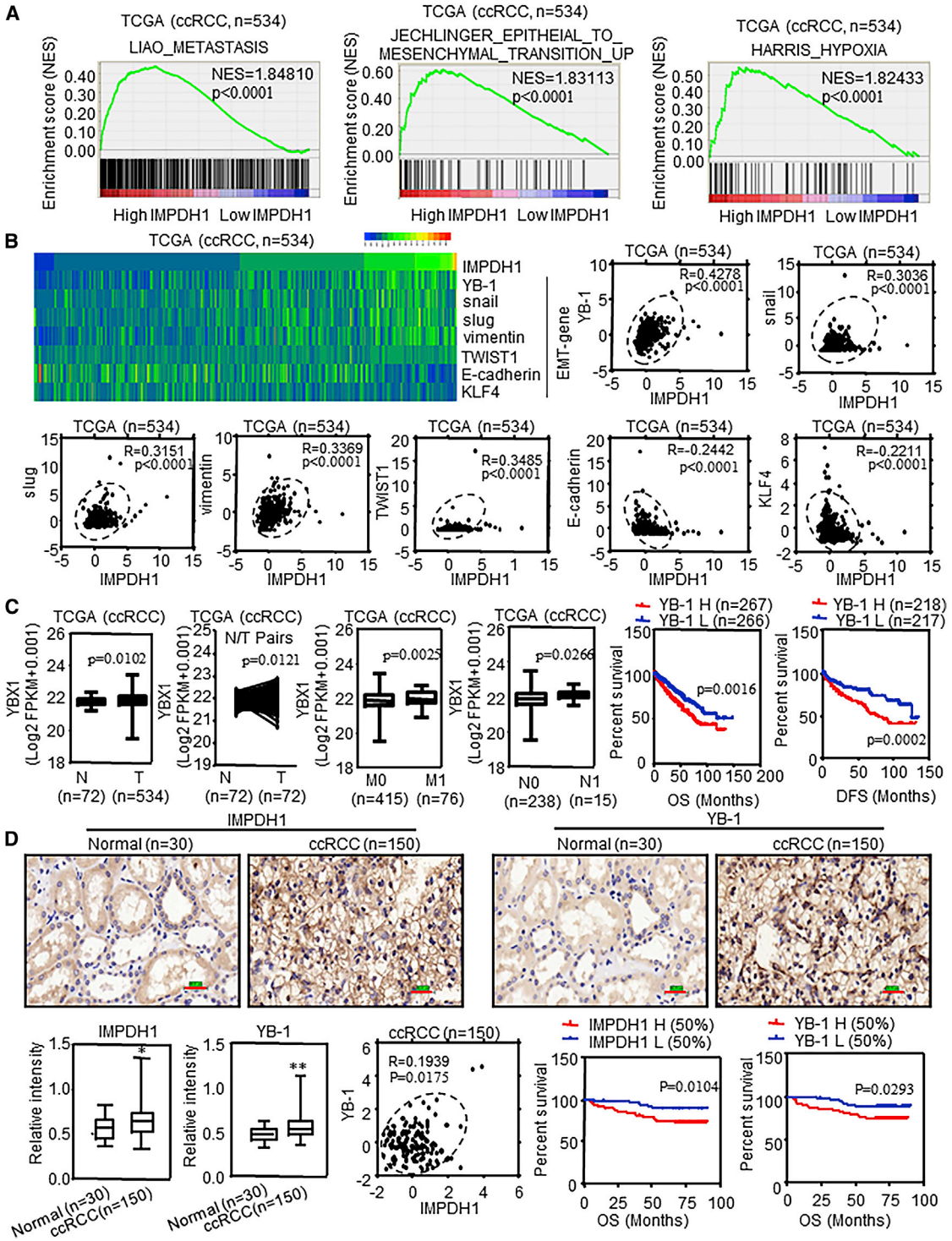

Figure 2. IMPDH1 Expression Positively Correlates with EMT Markers and YB-1 Expression in ccRCC

(A) GSEA analysis of IMPDH1 mRNA levels and ccRCC signaling pathways. (B) Heatmap depicting the association of IMPDH1 with YB-1, epithelial markers, and mesenchymal markers. (C) YB-1 mRNA levels were significantly elevated in TCGA dataset composed of 534 ccRCC cases, including 72 paired cases (N, normal tissues; T, tumor tissues; M0, M0 stage; M1, M1 stage; N0, N0 stage; N1, N1 stage). Kaplan-Meier analysis of YB-1 in ccRCC patients for OS and DFS. (D) The immunohistochemical (IHC) staining of ccRCC TMA revealed that IMPDH1 ($p < 0.05$) and YB-1 ($p < 0.01$) levels were all significantly higher in ccRCC tissues (scale bars, 50 μm). IMPDH1 levels were positively correlated with YB-1 ($R = 0.1939$, $p = 0.0175$). Kaplan-Meier analysis of IMPDH1 and YB-1 in ccRCC patients for OS ($p = 0.0104$, $p = 0.0293$). $^{**}p < 0.01$, $^{*}p < 0.05$.

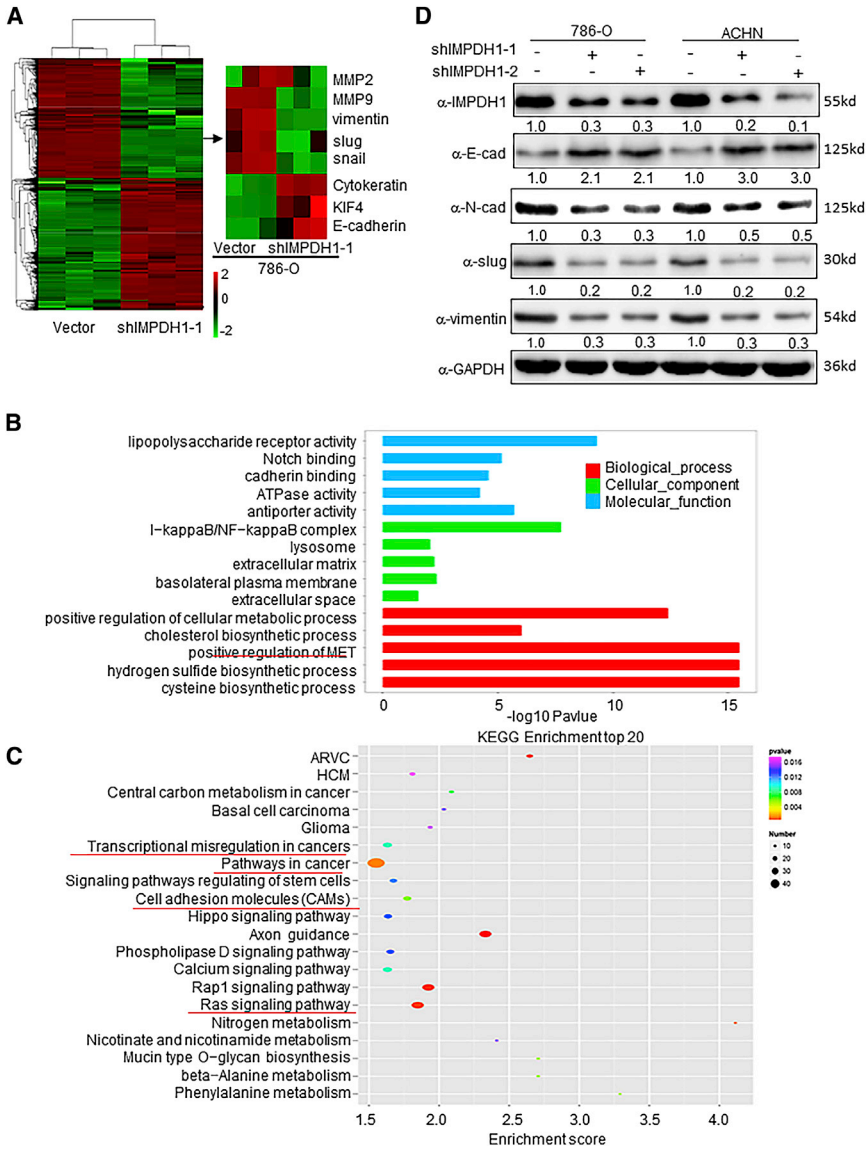

Figure 3. IMPDH1 Positively Regulates Metastasis and the EMT Signaling Pathway in ccRCC

(A) Our mRNA sequencing results showed that knockdown of IMPDH1 upregulated epithelial markers and downregulated mesenchymal markers in 786-O cells. (B) The GO analysis showed that IMPDH1 knockdown could positively regulate the process of MET. (C) The downregulated gene-enriched KEGG pathways in the mRNA sequencing results. (D) IMPDH1 knockdown increased levels of E-cadherin and reduced levels of N-cadherin, slug, and vimentin in 786-O and ACHN cells. The values indicate protein expression levels relative to GAPDH.

expression decreased in IMPDH1 knockdown cells, whereas YB-1 protein expression levels increased in cells overexpressing IMPDH1. However, sequencing results showed that IMPDH1 did not regulate YB-1 mRNA levels, suggesting that IMPDH1 might control YB-1 function by regulating stability of the YB-1 protein. We used MG132, a proteasome inhibitor, to investigate the mechanisms involved in IMPDH1-dependent YB-1 stabilization. Treatment of IMPDH1 knockdown 786-O cells with MG132 increased YB-1 protein accumulation (Figure 4B), indicating a constitutive YB-1 degradation in IMPDH1 knockdown 786-O cells. In addition, we also examined the effect of IMPDH1 on ubiquitin modification of YB-1 (Figure S4A). The results showed that IMPDH1 could inhibit the ubiquitination degradation of YB-1. Accordingly, cycloheximide (CHX) was used to inhibit protein synthesis in 786-O cells with stably knocked down IMPDH1, and YB-1 protein turnover was detected over time. In comparison to control cells, the half-life of YB-1 was dramatically reduced in 786-O cells with stably knocked down IMPDH1 (Figure 4C). Taken together, these observations indicated that IMPDH1 maintained the stabilization of the YB-1 protein.

Bioinformatics analysis showed that IMPDH1 levels were positively correlated with YB-1 expression in ccRCC. To validate the relevance of IMPDH1 and YB-1, we successfully constructed the 786-O and ACHN cell lines with stably knocked down or overexpressed YB-1. qPCR results showed that YB-1 positively regulated mRNA levels of IMPDH1 in 786-O and ACHN cells (Figure S4B). We also found that the protein expression of IMPDH1 was decreased after YB-1 knockdown, whereas IMPDH1 levels were increased after YB-1 overexpression (Figure 4D). It has been previously shown that YB-1 can bind to target gene promoters at the Y-box sequence (CAAT/ATTG).[27] To further clarify the mechanism of YB-1 in the regulation of IMPDH1, we found that the human IMPDH1 proximal promoter region (−1 to −1.5 kb upstream of the transcription start site [TSS]) had five YB-1 putative binding sites that could be bound and activated by YB-1 (Figure 4E). To verify the regulation of IMPDH1 by YB-1, we performed luciferase reporter assays with the wild-type (WT) IMPDH1 promoter (−1 to −1.5 kb) and mutant IMPDH1 promoter (deletions of the YB-1 putative binding sites). As shown in Figure 4E, YB-1 overexpression promoted WT rather than mutant luciferase reporter activity in 786-O and ACHN cells, indicating that YB-1 might bind to IMPDH1 through the binding sites of the promoter regions. Moreover, chromatin immunoprecipitation (ChIP) was performed in ACHN cells and indicated that YB-1 could activate IMPDH1 transcription and that YB-1 could bind to the designated regions of the IMPDH1 promoter (P3: −589 to −720 and P4: −675 to −830, containing the Y-box) (Figure 4F). Taken together, these results suggested that IMPDH1 and YB-1 formed a positive feedback loop: IMPDH1 maintained YB-1 protein stabilization; YB-1 induced IMPDH1 expression by binding to the IMPDH1 promoter motif.

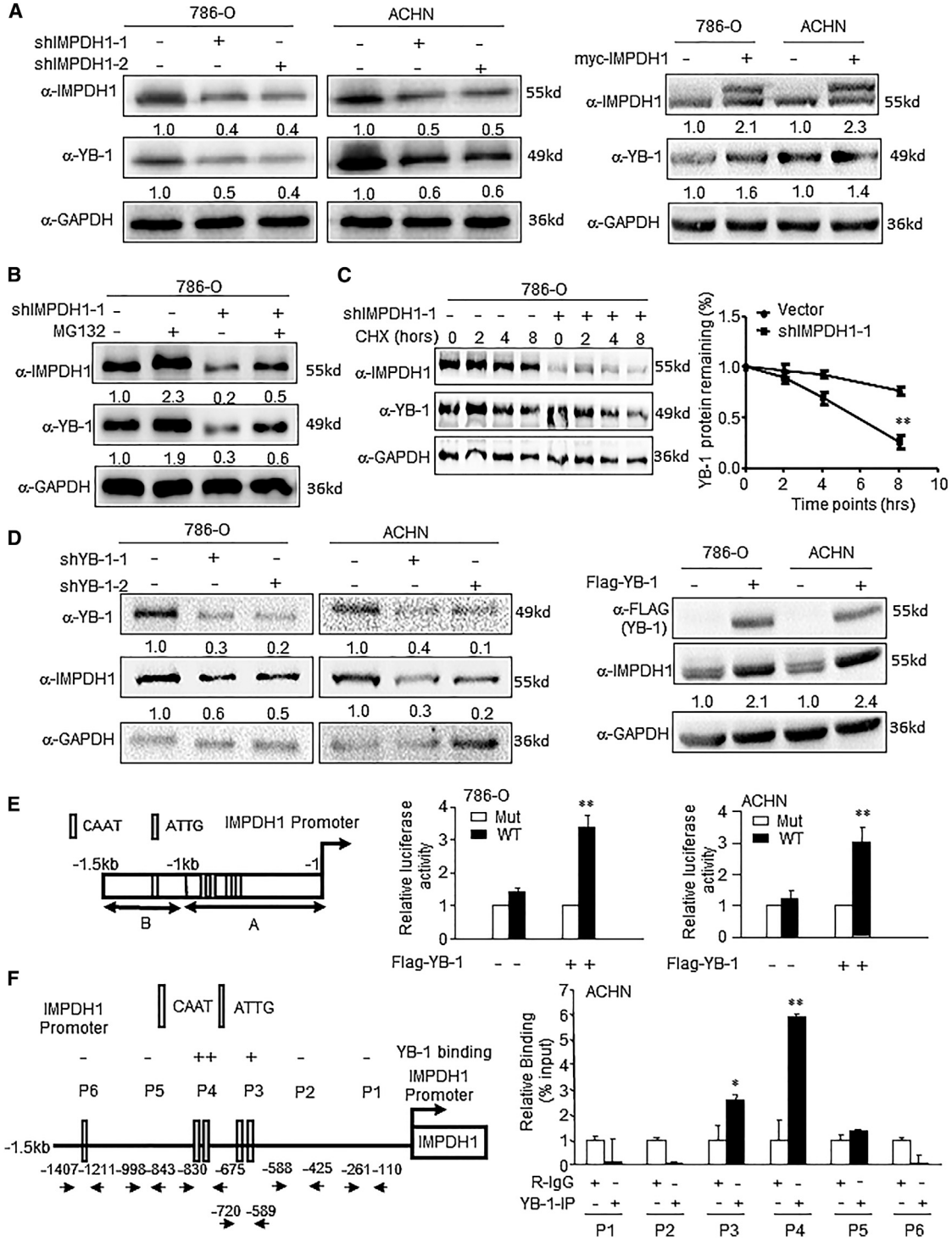

Figure 4. IMPDH1 and YB-1 Regulate Each Other and Form a Positive Feedback Loop

(A) Western blot analysis of YB-1 and IMPDH1 proteins in 786-O and ACHN cells with IMPDH1 knockdown and overexpression. The values indicate protein expression levels relative to GAPDH. (B) YB-1 protein accumulation was analyzed after treatment with MG132 in 786-O cells. The values indicate protein expression levels relative to GAPDH. (C) After cycloheximide (CHX) treatment, the half-life of YB-1 protein was analyzed in 786-O cells (vector and shIMPDH1). (D) Western blot analysis of YB-1 and IMPDH1 proteins in 786-O and ACHN cells with YB-1 knockdown and overexpression. The values indicate protein expression levels relative to GAPDH. (E) The human IMPDH1

(legend continued on next page)

IMPDH1-Assembled Cytoophidia Physically Interact with YB-1 and Translocate YB-1 into the Cell Nucleus

Immunohistochemical staining of ccRCC tissue microarray (TMA) and the cytoplasm and nuclear protein extraction experiments showed that both IMPDH1 and YB-1 were predominantly localized in the cytoplasm (Figures 2D and S5A), and IMPDH1 could maintain the stabilization of the YB-1 protein. We further explored whether IMPDH1 could bind to YB-1. Therefore, we performed protein immunoprecipitation (IP) experiments. To confirm the binding of IMPDH1 and YB-1, 786-O and ACHN cells were used to explore the binding of endogenous YB-1 to IMPDH1. As shown in Figure 5A, YB-1 was immunoprecipitated from cell lysates, and endogenous IMPDH1 was examined with anti-IMPDH-1 antibody by western blot analysis in anti-YB-1 pull-down lysates. We found that YB-1 coimmunoprecipitated with IMPDH1. Vice versa, IMPDH1 was immunoprecipitated from cell lysates, and endogenous YB-1 was examined with anti-YB-1 antibody by western blot analysis in anti-IMPDH1 pull-down lysates. We found that IMPDH1 also coimmunoprecipitated with YB-1 (Figure 5B). To further identify the domain of IMPDH1 that binds to YB-1 and the domain of YB-1 that binds to IMPDH1, we constructed truncated structures of IMPDH1 and YB-1 according to previous studies.[9,28] First, we examined the binding of the IMPDH1 truncation structure to YB-1. The glutathione S-transferase (GST)-IMPDH1 WT and GST-IMPDH1 (deletion of 108–245 amino acids [aa]) with FLAG-YB-1 proteins were purified for GST-pull-down and western blot assays to examine the direct binding of IMPDH1 and YB-1 proteins *in vitro*. As shown in Figure 5C, the constructs of GST-IMPDH1 (deletion of 108–245 aa) could not bind YB-1. We also found that GST-IMPDH1 WT coimmunoprecipitated with FLAG-YB-1 (Figure 5C), indicating that construct capable of assembling cytoophidia was sufficient for YB-1 binding. Then, FLAG-YB-1 WT, FLAG-YB-1 C-terminal (C-term; residues 129–324 aa), or FLAG-CSD (residues 51–128 aa) with myc-IMPDH1 WT were cotransfected into HEK293T. We observed that FLAG-YB-1 WT and FLAG-YB-1 C-term coimmunoprecipitated with myc-IMPDH1 (Figure 5D). We also tested the binding of another subtype of IMPDH, IMPDH2, to YB-1, and the results showed that IMPDH2 could not bind to YB-1 (Figure S5B). These findings suggested that only IMPDH1 physically interacted with YB-1.

The previous results have shown that the ratio of IMPDH1-assembled cytoophidia in the nucleus increased in the metastatic ccRCC tissues (Figure 1E), and the anti-IMPDH1 staining immunofluorescence results further confirmed that the IMPDH1-assembled cytoophidia could enter the nucleus (Figure S6A). Protein binding between IMPDH1 and YB-1 suggested that IMPDH1-assembled cytoophidia might translocate YB-1 into the nucleus, affecting YB-1 downstream gene expression, thus promoting the tumor metastasis. To verify this possibility, we performed immunofluorescence double staining with anti-IMPDH1 and anti-YB-1 in 786-O and ACHN cells in the presence or absence of mycophenolic acid (MPA). MPA treatment induced only IMPDH-assembled cytoophidia. As shown in Figures 5E, S6C, and S6D, IMPDH1 typically bound to YB-1 in the cytoplasm, whereas when IMPDH1 was assembled into cytoophidia, YB-1 could bind to cytoophidia and partially enter the nucleus. To further confirm that IMPDH1 cytoophidia drive YB-1 into the nucleus, we examined the proportion of YB-1 into the nucleus between the IMPDH1 knockdown group and the control group in the case of MPA induction. As shown in Figure 5F, knockdown of IMPDH1 significantly reduced the proportion of nuclear YB-1 proteins in the presence of IMPDH1-assembled cytoophidia. The localization of IMPDH1 and YB-1 was shown by immunofluorescence staining after IMPDH1 overexpression or knockdown with/without MPA treatment or with/without YB-1 overexpression (Figure S6B). Moreover, we performed immunoprecipitation with an anti-IMPDH1 antibody and analyzed YB-1 binding by western blot experiments in the presence or absence of MPA. As shown in Figure 5G, in the presence of MPA, IMPDH1 could bind more YB-1 protein. Furthermore, the results of immunoprecipitation with cytoplasm and nuclear protein extraction indicated that more interaction between IMPDH1 and YB-1 occurred in the nucleus under MPA treatment (Figure S6E). Taken together, these findings suggested that IMPDH1-assembled cytoophidia translocated YB-1 into the cell nucleus, thus correlating with the tumor metastasis.

IMPDH1 Promotes Tumor Cell Invasion and Migration through YB-1 Signaling

Previous studies have shown that YB-1 promotes tumor metastasis.[15,16] In the present study, IMPDH1-assembled cytoophidia could translocate YB-1 protein into the cell nucleus. Therefore, we first assessed whether cytoophidia in ccRCC affected tumor metastasis. As shown in Figure 6A, treatment of 786-O and ACHN cells with MPA promoted tumor cell migration and invasion, indicating that cytoophidia are involved in the regulation of tumor metastasis. Moreover, we transfected Myc-IMPDH1 WT, Myc-IMPDH1 (deletion of 108–245 aa), and vector into 786-O cells. As shown in Figure S7A, after MPA stimulation, immunofluorescence staining with Myc antibody showed that cells transfected with Myc-IMPDH1 (deletion of 108–245 aa) were unable to form cytoophidia. Transwell experiments showed that the Myc-IMPDH1 WT group had a stronger migration and invasion ability compared to Myc-IMPDH1 (delete 108–245 aa) and the vector group, whereas Myc-IMPDH1 (delete 108–245 aa) and the vector group have similar effects of cell migration and invasion (Figure S7A), indicating that the assembly of cytoophidia is correlated with cell migration and invasion *in vitro*. To further verify the function of cytoophidia, we constructed an *in vivo* metastatic model of ccRCC cytoophidia in nude mice by oral administration of MPA. In agreement with the *in vitro* experimental results, the cytoophidia were correlated with liver metastasis of ccRCC *in vivo* (Figure S8A). To illustrate whether cytoophidia promote metastasis by mediating IMPDH1, two or more independent

proximal promoter region (−1 to −1.5 kb upstream of the transcription start site [TSS]) had five Y-box sequences (CAAT/ATTG). IMPDH1 promoter reporters (−1 to −1.5 kb) were assessed in 786-O and ACHN cells. (F) ChIP analysis of YB-1 for the IMPDH1 promoter region in ACHN cells. ChIP assays were performed using an anti-YB-1 antibody. The error bars indicate the mean ± SEM of three independent assays. $^{**}p < 0.01$, $^{*}p < 0.05$.

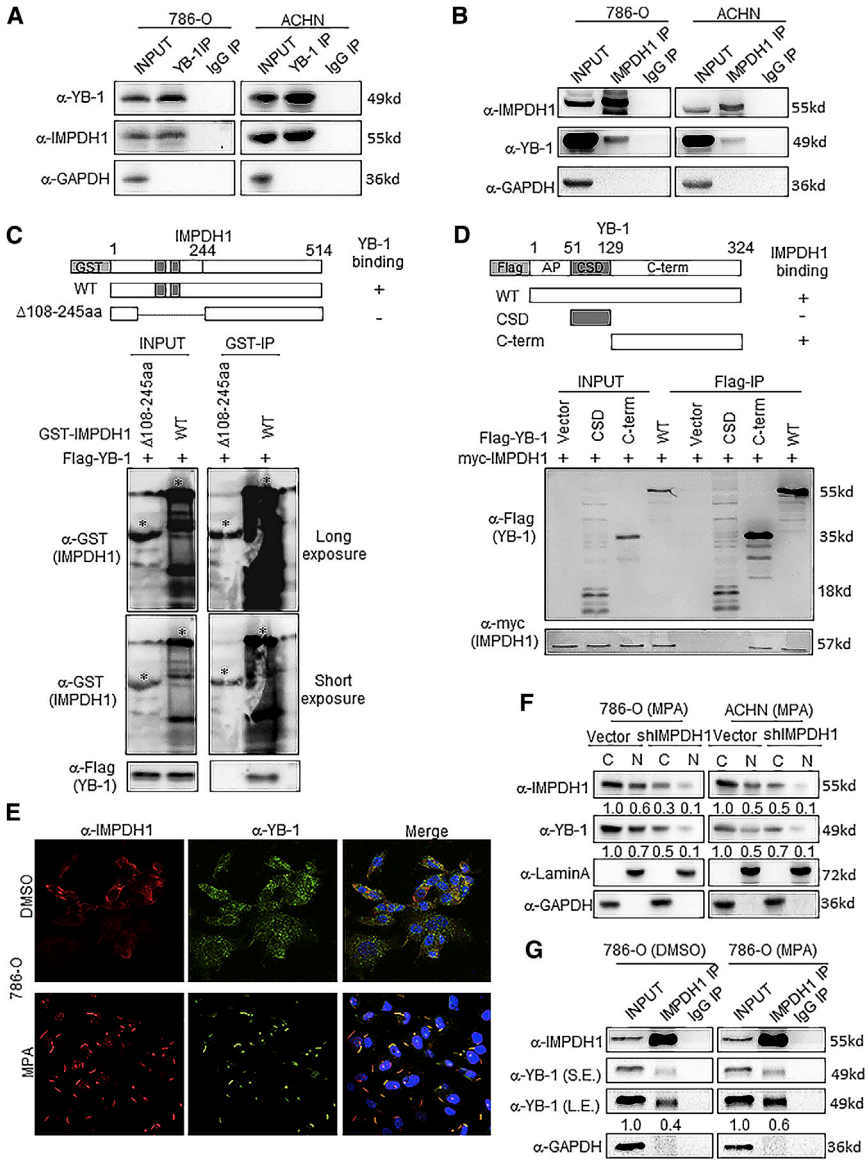

Figure 5. IMPDH1-Assembled Cytoophidia Physically Interact with YB-1 and Translocate YB-1 into the Cell Nucleus

(A) Immunoprecipitation (IP) experiments revealed that YB-1 protein coimmunoprecipitated with IMPDH1. (B) IP experiments revealed that IMPDH1 protein coimmunoprecipitated with YB-1. (C) Schematic representation of IMPDH1 and IMPDH1 truncated expression vectors. GST pull-down was performed with GST-IMPDH1 construct proteins and FLAG-YB-1 proteins. (D) Schematic representation of YB-1 and YB-1 truncated expression vectors. IP-western blot analysis was performed using 293T cells cotransfected with expression vectors encoding myc-tagged IMPDH1 and FLAG-tagged YB-1 truncated expression vectors. (E) Immunofluorescence staining analysis of IMPDH1-assembled cytoophidia. (F) Western blot analysis of cytoplasm and nuclear expression of IMPDH1 and YB-1 in 786-O and ACHN cells after MPA stimulation (C, cytoplasm; N, nuclear). (G) IP-western blot analysis of the binding of IMPDH1 and YB-1 in 786-O cells after MPA or DMSO stimulation (S.E., short exposure; L.E., long exposure).

shRNA plasmids were used, resulting in efficient knockdown of IMPDH1 in 786-O and ACHN cells (Figures 6B and S8B). IMPDH1 knockdown significantly reduced cytoophidia-mediated cell migration and invasion (Figures 6B and S8B). To further confirm the function of IMPDH1, we infected 786-O and ACHN cells with lentiviral vectors overexpressing IMPDH1, resulting in overexpression of IMPDH1 (Figures 6C and S8C). IMPDH1 overexpression clearly enhanced cytoophidia-mediated cell migration and invasion (Figures 6C and S8C). We have also examined the effect of IMPDH1 knockdown without MPA treatment and found that IMPDH1 knockdown inhibited cell migration and invasion *in vitro* (Figure S8D). These results indicated that cytoophidia functioned as a metastatic promoter by mediating IMPDH1. We speculated that the specific mechanisms by which IMPDH1 promoted ccRCC mobility might occur via IMPDH1 translocation of YB-1 into the nucleus to affect tumor metastasis. To verify this conjecture, we performed a rescue experiment by overexpressing YB-1 protein in IMPDH1 knockdown cells in the presence of MPA. As shown in Figure 6D, YB-1 overexpression could recover the pro-metastatic function of IMPDH1. However, the pro-metastatic function of IMPDH1 was abolished by YB-1 knockdown (Figure S8E). Taken together, these findings suggested that IMPDH1 promoted tumor cell invasion and migration through YB-1 signaling.

IMPDH1 Promotes Tumor Metastasis *In Vivo*

Our aforementioned results confirmed that IMPDH1 promoted ccRCC cell invasion and migration through YB-1 signaling *in vitro*, which prompted us to verify whether YB-1 could recover the function of IMPDH1 *in vivo*. Next, we constructed stable ccRCC cells by cotransfecting lentiviral particles with the shIMPDH1 plasmid (or negative control) and lentiviral particles carrying the FLAG-YB-1 plasmid (or negative control) into 786-O cells. Stable cells were then injected into the tail vein of nude mice, and MPA was orally administered to nude mice. Crucially, *in vivo* animal-live imaging revealed that YB-1 could recover the IMPDH1-mediated tumor metastasis (Figure 7A). Positron emission tomography (PET)-computed tomography (CT) scans of nude mice confirmed the results of animal-live imaging experiments (Figure 7B). We isolated the liver of nude mice for hematoxylin and eosin (H&E) staining and found that YB-1 could recover liver metastasis (white circles) mediated by the IMPDH1-assembled cytoophidia (Figure 7B). In addition, we found the formation of cytoophidia in the liver

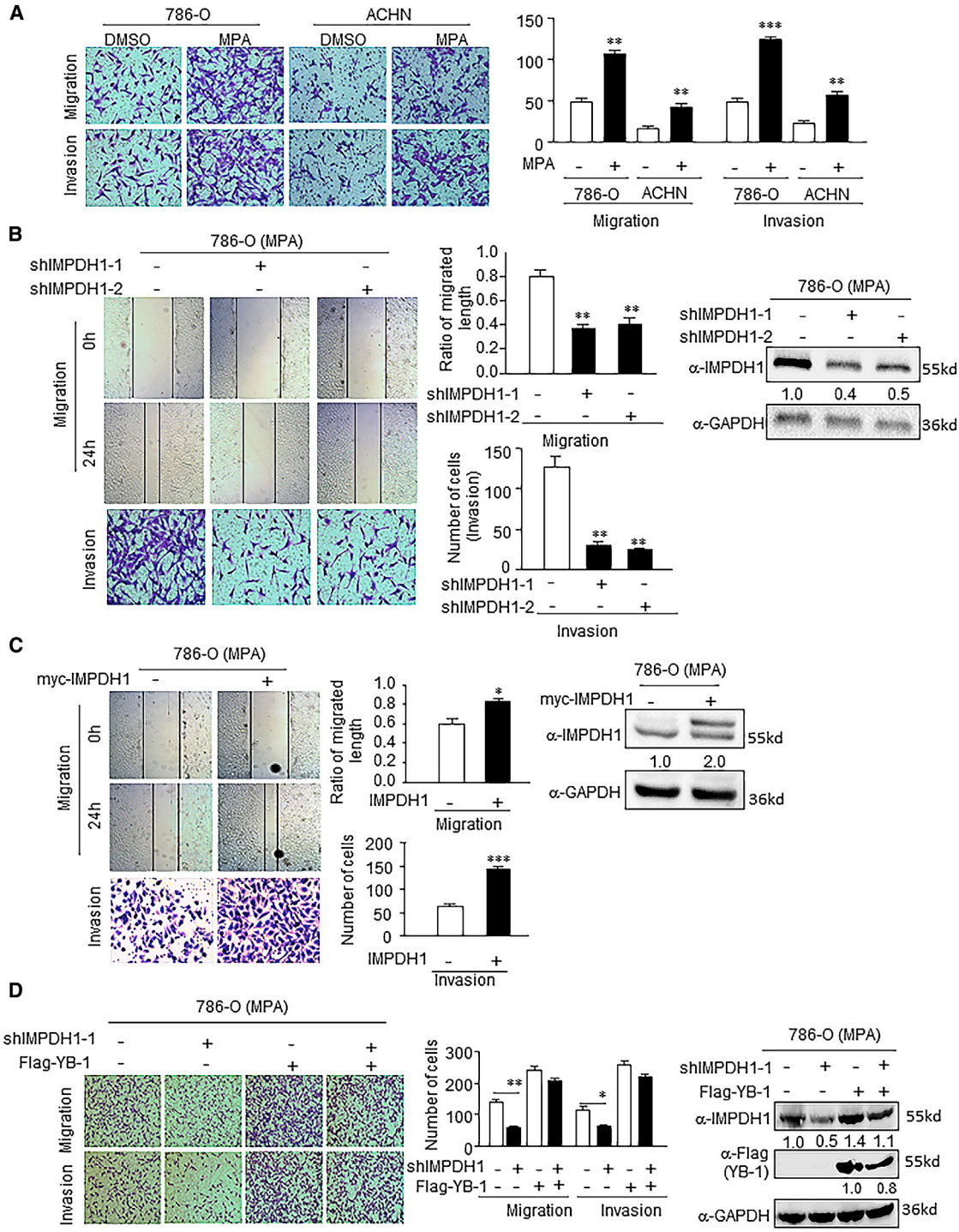

Figure 6. IMPDH1 Promotes Tumor-Cell Migration and Invasion through YB-1 Signaling *In Vitro*

(A) 786-O and ACHN cells treated with DMSO or MPA, cell migration, and invasion were analyzed by transwell assays. (B) IMPDH1 knockdown significantly reduced cell migration and invasion in 786-O cells. The values indicate protein expression levels relative to GAPDH. (C) IMPDH1 overexpression clearly enhanced cell migration and invasion in 786-O cells. The values indicate protein expression levels relative to GAPDH. (D) Rescue assays revealed that YB-1 overexpression could recover the pro-metastatic function of IMPDH1 in 786-O cells. The values indicate protein expression levels relative to GAPDH. The error bars indicate the mean ± SEM of three independent assays. ***$p < 0.001$, **$p < 0.01$, *$p < 0.05$, compared with the corresponding control.

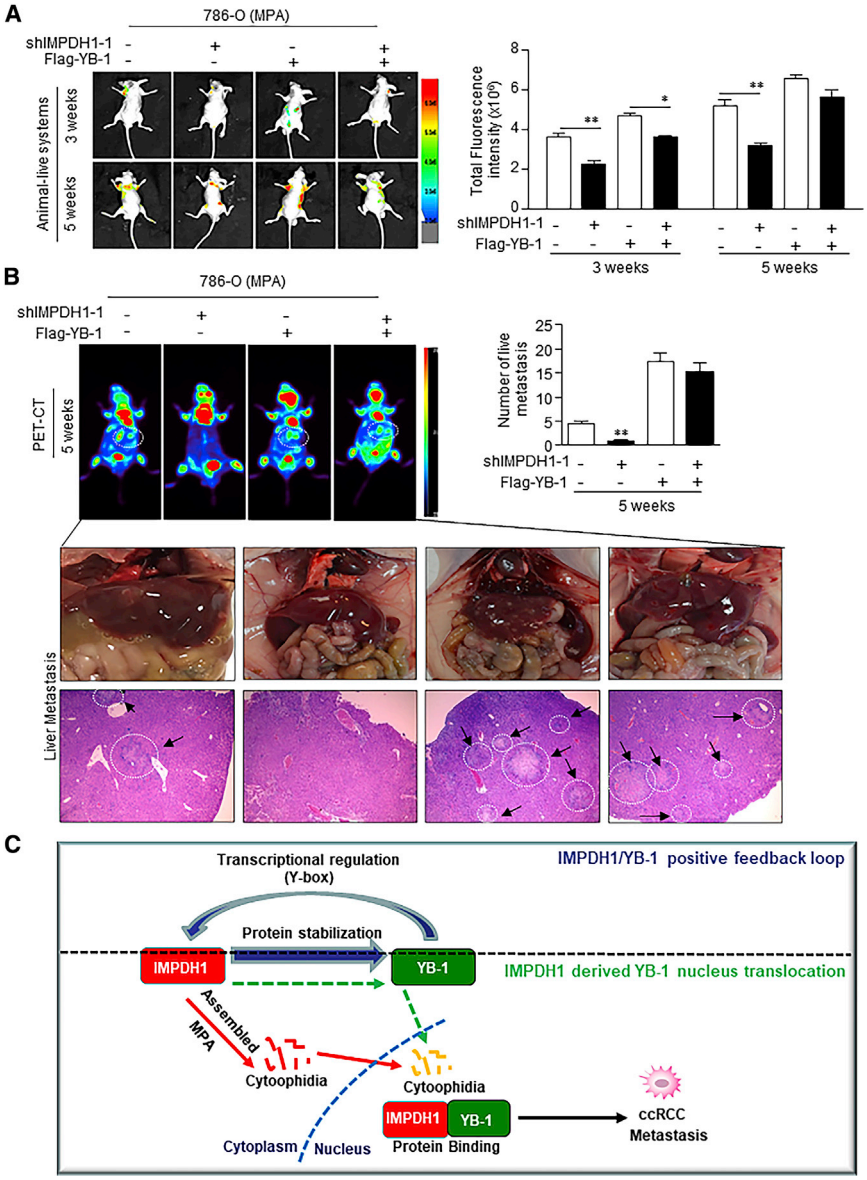

Figure 7. IMPDH1 Promotes Tumor Metastasis through YB-1 Signaling *In Vivo*

(A) *In vivo* animal-live imaging revealed that YB-1 could recover IMPDH1-mediated tumor metastasis in the 3rd and 5th weeks (n = 6 mice/group). (B) PET-CT scans of nude mice in the 5th weeks (white dashed circles indicate potential metastases). H&E staining of nude mouse liver (white dashed circles indicate potential metastases) (n = 6 mice/group). (C) Diagram of ccRCC metastasis mediated by IMPDH1/YB-1 positive feedback loop-assembled cytoophidia. $^{**}p < 0.01$, $^{*}p < 0.05$.

metastases of mice after oral administration of MPA (Figure S9A). Taken together, these results demonstrate that IMPDH1 promoted tumor metastasis through YB-1 signaling *in vivo*. Based on our *in vitro* and *in vivo* experimental results, we mapped the mechanisms of ccRCC metastasis mediated by the IMPDH1/YB-1 positive feedback loop (Figure 7C).

DISCUSSION

The cytoophidium assembled by CTPS was first discovered and described in *Drosophila* in 2010 by Liu.[4] Filamentous formation of CTPS was also confirmed in human cells.[8,29] Interestingly, IMPDH can also be assembled into filament-like structures that are very similar in appearance to the CTPS-assembled cytoophidium.[8] CTPS and IMPDH, which are key enzymes in nucleotide metabolism, can assemble into cytoophidia in human cells, both of which have two subtypes, termed CTPS1 and CTPS2 and IMPDH1 and IMPDH2, respectively.[26] Under normal culture conditions, IMPDH can form cytoophidia in approximately 30% of HEK293T cells, whereas CTPS can barely assemble cytoophidia.[30] 6-Diazo-5-oxo-l-norleucine (DON), a glutamine analog that blocks the biosynthesis of cytidine triphosphate (CTP) and guanosine-5′-triphosphate (GTP), or MPA, an IMPDH inhibitor, prompted the assembly of the cytoophidia in human cells.[31] After DON or MPA treatment, IMPDH- and CTPS-assembled cytoophidia were observed in more than 90% of cells.[30] A recent study[11] has shown that cytoophidia naturally exist in various human cancer tissues. However, biological behaviors and functions of cytoophidia in cancers are exceptionally attractive but have not yet been thoroughly explored. In the present study, IMPDH-assembled cytoophidia naturally existed in ccRCC tissues. However, only IMPDH1 expression showed a significant increase in protein and mRNA levels and correlated negatively with the OS and DFS of ccRCC patients. Additionally, we also found that the expression levels of IMPDH1 and YB-1 as well as the ratio of IMPDH1 and YB-1 in the nucleus were higher in mRCC tisssues. Moreover, the expression levels of IMPDH1 were positively correlated with YB-1 in mRCC tissues. IMPDH1 is an independent prognostic risk factor in ccRCC. Thus, we focused our research on IMPDH1-assembled cytoophidia in ccRCC. We found that the number of IMPDH1-assembled cytoophidia and the ratio of IMPDH1-assembled cytoophidia in the nucleus increased in the metastatic ccRCC tissues. IMPDH1-assembled cytoophidia correlated with ccRCC metastasis via the YB-1 signaling pathway. Our findings identified, for the first time, the biological behaviors and functions of cytoophidia in cancer.

YB-1, as a DNA/RNA binding protein, regulates the expression of downstream genes at the transcriptional or translational level. YB-1

promotes EMT by activating the translation of Snail1 and other regulated transcription factors in breast cancer[15] and facilitates sarcoma metastasis by activating the translation of HIF1α.[16] Knockdown of YB-1 inhibits the invasion of melanoma cells *in vitro*.[32] These studies consistently demonstrate that YB-1 promotes tumor cell metastasis in various cancers. Interestingly, in this study, we used GSEA to analyze gene sets that were altered by IMPDH1 and YB-1 expression in the ccRCC TCGA dataset. Our results showed that metastasis, EMT, and hypoxia signaling pathways were all positively associated with both IMPDH1 and YB-1 expression. IMPDH1 expression was positively correlated with YB-1 expression. Mechanistically, IMPDH1 and YB-1 formed an autoregulatory positive feedback loop in ccRCC: IMPDH1 maintained YB-1 protein stabilization; YB-1 induced IMPDH1 expression by binding the IMPDH1 promoter motif. Furthermore, IMPDH1 physically interacted with YB-1, and the IMPDH1-assembled cytoophidia translocated YB-1 into the cell nucleus. Given the high sequence similarity between IMPDH1 and IMPDH2, we performed a co-IP experiment and found that IMPDH2 cannot bind to YB-1. Moreover, the expression levels of IMPDH2 were not upregulated in renal cancer cells. Functionally, the assembly of IMPDH1 cytoophidia correlated with ccRCC cell invasion and migration via the YB-1 signaling pathway. Our findings provide, for the first time, a solid theoretical rationale for targeting the IMPDH1/YB-1 axis to improve metastatic renal cancer treatment.

The cytoophidium is a new frontier in the field of cell biology. At present, the study of cytoophidia is still in its infancy, with many previously unexplored questions remaining unanswered. Our study findings confirm, for the first time, that IMPDH1-assembled cytoophidia correlated with tumor metastasis, enriching our understanding of the function of cytoophidia in the field of human tumors. In the future, our team will continue to explore the possible functions of cytoophidia in tumors, including cytoskeletal-like functions, metabolic control, metabolic buffering, protein stabilization, cell proliferation, developmental switching, coping with stress, metabolic channeling, intracellular transport, and nuclear compartmentation.[10]

At present, the clinical occurrence rate of classical renal cancer triplet syndrome (hematuria, backache, and abdominal mass) in patients with renal cancer has been less than 15%. These patients often have advanced renal cancer at the time of diagnosis. Early detection and diagnosis of asymptomatic renal cancer will lead to better treatment outcomes.[33] Therefore, the diagnostic biomarkers for renal cancer have become a hot topic of research. ccRCC, the most common subtype of RCC, has been reported to have multiple diagnostic biomarkers, including recoverin, vimentin, EMA, CK18, CD10, caveolin-1, S100, PAX2, PAX8, and CA9.[34–39] Among these markers, the upregulation of PAX2 and CD10 has been reported to be due to inactivation of VHL in ccRCC.[40] In the present study, we generated a ROC curve to analyze the diagnostic value of IMPDH1 for ccRCC in 72 paired cases from the ccRCC TCGA database. Our results demonstrated that IMPDH1 could effectively distinguish ccRCC patients from normal tissues. These results suggest that IMPDH1 may have potential as a new diagnostic biomarker for renal cancer. The results of this study indicate that IMPDH1-assembled cytoophidia are naturally present in ccRCC tissues and correlated with tumor metastasis. Therefore, we hypothesize that IMPDH1 may be indicators of ccRCC metastasis.

In the current studies, our cytoophidia model is based on the premise of MPA processing. There is currently no direct evidence to support that knockdown or overexpression of IMPDH1 causes cytoophidium disassembly or assembly. At present, the function of cytoophidia in the tumor cells has not been reported, and there is no natural cytoophidia model for cell researching. Our future studies will focus on the establishment of a more effective cytoophidia model.

In general, we identified a mechanical and functional link between IMPDH1-assembled cytoophidia and YB-1 in ccRCC. Our study provides, for the first time, convincing evidence that functional inhibition of the IMPDH1/YB-1 positive feedback loop and disassembly of cytoophidia are new targets for the treatment of metastatic renal cell carcinoma.

MATERIALS AND METHODS

The ccRCC Tissue Samples

Human ccRCC TMAs were purchased from Outdo Biotech (XT15-050). All clinical and pathological information, including pathological diagnosis, clinical stage, pathological stage, and survival data, can be viewed directly on the website (http://www.superchip.com.cn/index.html).

We collected 50 pairs of ccRCC and normal adjacent tissues from Wuhan Union Hospital between 2014 and 2015. Resected tissues were immediately collected and stored in liquid nitrogen. Before surgery, none of the patients had received any chemotherapy or radiotherapy or targeted therapies or immunotherapy. All patients signed an informed consent form. These studies were conducted in compliance with approved guidelines. All experimental procedures were approved by the Human Ethics Committee of Huazhong University of Science and Technology.

Cell Culture, Infection, Transfection, Plasmid Construction, and Reagents

The human renal cancer cell lines ACHN, 786-O, Caki-1, and A498 and renal normal epithelial cell line HK-2 were purchased from The American Type Culture Collection. Cell culture was performed as previously described.[41] shRNA against IMPDH1 (shIMPDH1), YB-1 (shYB-1), IMPDH2 (shIMPDH2), and the corresponding control (sh-ctr) with nonsense sequences were constructed by Shanghai Genechem. The pGV341-FLAG-YB-1 (YB-1), pGV492-MYC-IMPDH1 (IMPDH1), and empty vector (vector) were constructed by Shanghai Genechem. The lentiviral particles containing pGV341-FLAG-YB-1, pGV492-MYC-IMPDH1, pGV248-shYB-1, and pGV248-shIMPDH1 were constructed by Shanghai Genechem and used to infect 786-O or ACHN cells, according to the

manufacturer's recommendations. The Myc-IMPDH1 (delete 108–514 aa) was constructed by Vigene Biosciences (Shan Dong, China). Briefly, the truncated plasmid construction methods were as follows: the target gene fragments were amplified by PCR, and the GV140 vectors were cleaved by XhoI/EcoRI enzymes; finally, the PCR amplification products were recombined with these vectors. p-FLAG-YB-1-CSD and p-FLAG-YB-1-C-term were kindly provided by K.C. (Wuhan Union Hospital). Plasmids were transfected with Lipofectamine 2000, according to the manufacturer's recommendations. MPA was purchased from Sigma-Aldrich. MG132 was purchased from Selleck Chemicals (Houston, TX, USA). CHX was purchased from MedChemExpress (MCE; USA).

Immunohistochemistry and Immunofluorescence Assays

Immunohistochemical analysis of human renal carcinoma tissues was performed using a polyclonal IMPDH1 antibody (22092-1-AP, Proteintech, China; ab55297, Abcam) and a polyclonal YB-1 antibody (20339-1-AP; Proteintech, China). Specific experiments were performed as previously described.[42,43] For the immunofluorescence experiments, cells were fixed in 4% paraformaldehyde, permeabilized with 0.3% Triton X-100, and blocked with 3% BSA for 1 h at 37°C, followed by incubation with primary antibody and fluorescent secondary antibodies. The immunostaining quantification methods were to count the number of cytoophidia entering into the nucleus in each field of view and then take the average of three fields of view. The presentation of the histogram was the result of three independent experiments.

Immunoprecipitation and Western Blotting Assays

IP experiments were performed in 786-O, ACHN, and HEK293T cells, as indicated. Cells were resuspended and lysed in Triton lysis buffer (TLB) containing the protease inhibitors PMSF and cocktail. We used 2% of the lysate as input, and the rest was used for IP. Antibodies for western blotting and IP were as follows: anti-IMPDH1 (22092-1-AP; Proteintech, China), anti-YB-1 (sc-101198; Santa Cruz Biotechnology), anti-IMPDH1 (ab55297; Abcam), anti-FLAG (66008-2-immunoglobulin [Ig], 20543-1-AP; Proteintech, China), anti-MYC (BM0238, BM4042; Boster), anti-glyceraldehyde 3-phosphate dehydrogenase (GAPDH; sc-47724; Santa Cruz Biotechnology), anti-E-cadherin (20874-1-AP; Proteintech, China), anti-N-cadherin (ab18203; Abcam), anti-slug (12129-1-AP; Proteintech, China), anti-vimentin (10366-1-AP; Proteintech, China), anti-IMPDH2 (12948-1-AP; Proteintech, China), and anti-lamin A (sc-293162; Santa Cruz Biotechnology).

Direct Protein Binding by GST Pull-Down Assays

Direct binding of proteins *in vitro* was performed as previously described.[44]

Luciferase Reporter Assays

WT and mutant IMPDH1 promoter reporter and control plasmid were constructed by Genechem. Renilla luciferase reporter, WT, and mutant IMPDH1 promoter reporter were cotransfected into cells overexpressing YB-1 or vector using Lipofectamine 2000. Luciferase activities were measured after 48 h of transfection using Renilla luciferase for normalization.

ChIP Assays

ChIP assays were performed as previously described.[45] The primer sequences for the IMPDH1 promoter region were as follows:

P1 (−110∼−261): 3′-GAAGGGGCCAGGAGACAC-5′, 3′-AGATGCCTAGACTCGGTTCG-5′;

P2 (−425∼−588): 3′-CACTCCCTTGTTACGGGGTA-5′, 3′-GCCGACTCCACGTTAGAGAG-5′;

P3 (−589∼−720): 3′-CCTGAGGGCAAGGACTCTTA-5′, 3′-GGGCAGAGCAGTGTACTCAA-5′;

P4 (−675∼−830): 3′-TCCATCTGTAAGGTTGAAAAATC-5′, 3′-CACCTAGCAAAAATGGCAAA-5′;

P5 (−843∼−998): 3′-AGCTTGCAGTGAGCCGAGAT-5′, 3′-CCTGAGGTAGCCCCATCTTT-5′;

P6 (−1,211∼−1,407): 3′-TCTGGGGAGTGGGTGTGTAT-5′, 3′-GCGCATCTGGACTTTTGTCT-5′.

Monoclonal antibody against YB-1 (sc-101198; Santa Cruz Biotechnology) was used for IP, and normal IgG served as a negative control. We used 2% of the original DNA as a positive input control.

Bioinformatic Analysis

A standardized mRNA expression dataset for renal cancer was downloaded from the publicly available database TCGA and used to assess the expression and correlation of IMPDH1, YB-1, E-cadherin, N-cadherin, KLF4, vimentin, Snail1, and Twist1. This dataset was also used to evaluate OS and DFS in renal cancer patients. Spearman's correlation coefficient was calculated for the mRNA expression levels for all cancer samples. $p < 0.05$ was considered statistically significant. Oncomine, another public cancer database, was also used to mine IMPDH1 mRNA data.

Microarray Analysis

786-O cells knocked down for IMPDH1 or control were harvested 7 days after puromycin selection. Microarray analysis was performed on three duplicate samples by Shanghai OE Biotech. Differentially expressed genes between 786-O sh-vector and 786-O shIMPDH1 cells were selected based on a mean fold difference of 1.5 and the associated t test, with a p value < 0.05. The RNA sequence (RNA-seq) data have been deposited to GEO under the accession number GenBank: GSE146231.

Wound-Healing Assays and Transwell Migration and Invasion Assays

Wound-healing assays and transwell assays were performed as previously described.[46,47]

Quantitative Real-Time PCR Assays

Quantitative real-time PCR was performed as previously described.[48]

In Vivo Renal Cancer Metastasis Model

A total of 5×10^5 cells were injected via the tail vein into 4- to 5-week-old male nude mice purchased from Beijing HFK Bio-technology. Tumor metastasis lesions were measured using an animal-live imaging system and PET at the 3rd and 5th weeks, respectively. After the nude mice were sacrificed, the metastatic lesions were stained with H&E. For the cytoophidia metastasis model, 10 μM MPA was orally administered once every other day via a gavage needle after the cells were injected via the tail vein into nude mice. All animal experiments were approved by the Animal Ethics Committee of Tongji Medical College of Huazhong University of Science and Technology.

Statistical Analysis

The statistical analysis was performed using GraphPad Prism 6.0 (GraphPad Software, USA) or SPSS statistical software 22.0 (IBM SPSS, Chicago, IL, USA). Data are presented as the mean ± SEM. Statistical analyses were performed using Mann-Whitney test and Student's t test and the Pearson correlation coefficient. The Kaplan-Meier curve and log-rank test were used to assess the survival of patients. Statistical significance was determined when the p value was less than 0.05.

SUPPLEMENTAL INFORMATION

Supplemental Information can be found online at https://doi.org/10.1016/j.ymthe.2020.03.001.

AUTHOR CONTRIBUTIONS

Conceptualization and Design, K.C. and X.Z.; Acquisition of Data (conducted the experiments, provided animals, acquired and managed patients, etc.), H.R., Z.S., Q.C., D.N., T.X., K.W., L.B., J.T., H.X., and W.X.; Data Analysis, H.R., H.Y., G.C., Z.X., L.W., D.L., H.L., T.O., and B.H.J.; Writing, H.R., Z.S., and Q.C.; Supervision, K.C. and X.Z.

CONFLICTS OF INTEREST

The authors declare no competing interests.

ACKNOWLEDGMENTS

This study was supported by the National Natural Science Foundation of China (grant nos. 81874090, 81672528, 81672524, and 81472405); Hubei Provincial Natural Science Foundation of China (2018CFA038); Foundation of Health and Family Planning Commission of Hubei Province in China (WJ2017M124); Independent Innovation Foundation of Huazhong University of Science and Technology (118530309); Clinical Research Physician Program of Tongji Medical College, Huazhong University of Science and Technology (5001530015); and Integrated Innovation Team for Major Human Disease Program of Tongji Medical College, Huazhong University of Science and Technology.

REFERENCES

1. Ljungberg, B., Bensalah, K., Canfield, S., Dabestani, S., Hofmann, F., Hora, M., Kuczyk, M.A., Lam, T., Marconi, L., Merseburger, A.S., et al. (2015). EAU guidelines on renal cell carcinoma: 2014 update. Eur. Urol. *67*, 913–924.
2. Gupta, G.P., and Massagué, J. (2006). Cancer metastasis: building a framework. Cell *127*, 679–695.
3. Cutz, J.C., Guan, J., Bayani, J., Yoshimoto, M., Xue, H., Sutcliffe, M., English, J., Flint, J., LeRiche, J., Yee, J., et al. (2006). Establishment in severe combined immunodeficiency mice of subrenal capsule xenografts and transplantable tumor lines from a variety of primary human lung cancers: potential models for studying tumor progression-related changes. Clin. Cancer Res. *12*, 4043–4054.
4. Liu, J.-L. (2010). Intracellular compartmentation of CTP synthase in Drosophila. J. Genet. Genomics *37*, 281–296.
5. Ingerson-Mahar, M., Briegel, A., Werner, J.N., Jensen, G.J., and Gitai, Z. (2010). The metabolic enzyme CTP synthase forms cytoskeletal filaments. Nat. Cell Biol. *12*, 739–746.
6. Noree, C., Sato, B.K., Broyer, R.M., and Wilhelm, J.E. (2010). Identification of novel filament-forming proteins in Saccharomyces cerevisiae and Drosophila melanogaster. J. Cell Biol. *190*, 541–551.
7. Hedstrom, L. (2009). IMP dehydrogenase: structure, mechanism, and inhibition. Chem. Rev. *109*, 2903–2928.
8. Carcamo, W.C., Satoh, M., Kasahara, H., Terada, N., Hamazaki, T., Chan, J.Y., Yao, B., Tamayo, S., Covini, G., von Mühlen, C.A., and Chan, E.K. (2011). Induction of cytoplasmic rods and rings structures by inhibition of the CTP and GTP synthetic pathway in mammalian cells. PLoS ONE *6*, e29690.
9. Thomas, E.C., Gunter, J.H., Webster, J.A., Schieber, N.L., Oorschot, V., Parton, R.G., and Whitehead, J.P. (2012). Different characteristics and nucleotide binding properties of inosine monophosphate dehydrogenase (IMPDH) isoforms. PLoS ONE *7*, e51096.
10. Liu, J.L. (2016). The Cytoophidium and Its Kind: Filamentation and Compartmentation of Metabolic Enzymes. Annu. Rev. Cell Dev. Biol. *32*, 349–372.
11. Chang, C.C., Jeng, Y.M., Peng, M., Keppeke, G.D., Sung, L.Y., and Liu, J.L. (2017). CTP synthase forms the cytoophidium in human hepatocellular carcinoma. Exp. Cell Res. *361*, 292–299.
12. Toh, S., Nakamura, T., Ohga, T., Koike, K., Uchiumi, T., Wada, M., Kuwano, M., and Kohno, K. (1998). Genomic organization of the human Y-box protein (YB-1) gene. Gene *206*, 93–97.
13. Evdokimova, V., Ovchinnikov, L.P., and Sorensen, P.H. (2006). Y-box binding protein 1: providing a new angle on translational regulation. Cell Cycle *5*, 1143–1147.
14. Kohno, K., Izumi, H., Uchiumi, T., Ashizuka, M., and Kuwano, M. (2003). The pleiotropic functions of the Y-box-binding protein, YB-1. BioEssays *25*, 691–698.
15. Evdokimova, V., Tognon, C., Ng, T., Ruzanov, P., Melnyk, N., Fink, D., Sorokin, A., Ovchinnikov, L.P., Davicioni, E., Triche, T.J., and Sorensen, P.H. (2009). Translational activation of snail1 and other developmentally regulated transcription factors by YB-1 promotes an epithelial-mesenchymal transition. Cancer Cell *15*, 402–415.
16. El-Naggar, A.M., Veinotte, C.J., Cheng, H., Grunewald, T.G., Negri, G.L., Somasekharan, S.P., Corkery, D.P., Tirode, F., Mathers, J., Khan, D., et al. (2015). Translational Activation of HIF1α by YB-1 Promotes Sarcoma Metastasis. Cancer Cell *27*, 682–697.
17. Giménez-Bonafé, P., Fedoruk, M.N., Whitmore, T.G., Akbari, M., Ralph, J.L., Ettinger, S., Gleave, M.E., and Nelson, C.C. (2004). YB-1 is upregulated during prostate cancer tumor progression and increases P-glycoprotein activity. Prostate *59*, 337–349.
18. Mo, D., Fang, H., Niu, K., Liu, J., Wu, M., Li, S., Zhu, T., Aleskandarany, M.A., Arora, A., Lobo, D.N., et al. (2016). Human Helicase RECQL4 Drives Cisplatin Resistance in Gastric Cancer by Activating an AKT-YB1-MDR1 Signaling Pathway. Cancer Res. *76*, 3057–3066.
19. Chatterjee, M., Rancso, C., Stühmer, T., Eckstein, N., Andrulis, M., Gerecke, C., Lorentz, H., Royer, H.D., and Bargou, R.C. (2008). The Y-box binding protein YB-1 is associated with progressive disease and mediates survival and drug resistance in multiple myeloma. Blood *111*, 3714–3722.
20. Jurchott, K., Bergmann, S., Stein, U., Walther, W., Janz, M., Manni, I., Piaggio, G., Fietze, E., Dietel, M., and Royer, H.D. (2003). YB-1 as a cell cycle-regulated transcription factor facilitating cyclin A and cyclin B1 gene expression. J. Biol. Chem. *278*, 27988–27996.

21. Shibao, K., Takano, H., Nakayama, Y., Okazaki, K., Nagata, N., Izumi, H., Uchiumi, T., Kuwano, M., Kohno, K., and Itoh, H. (1999). Enhanced coexpression of YB-1 and DNA topoisomerase II alpha genes in human colorectal carcinomas. Int. J. Cancer *83*, 732–737.

22. Shiota, M., Takeuchi, A., Song, Y., Yokomizo, A., Kashiwagi, E., Uchiumi, T., Kuroiwa, K., Tatsugami, K., Fujimoto, N., Oda, Y., and Naito, S. (2011). Y-box binding protein-1 promotes castration-resistant prostate cancer growth via androgen receptor expression. Endocr. Relat. Cancer *18*, 505–517.

23. Bargou, R.C., Jürchott, K., Wagener, C., Bergmann, S., Metzner, S., Bommert, K., Mapara, M.Y., Winzer, K.J., Dietel, M., Dörken, B., and Royer, H.D. (1997). Nuclear localization and increased levels of transcription factor YB-1 in primary human breast cancers are associated with intrinsic MDR1 gene expression. Nat. Med. *3*, 447–450.

24. Kuwano, M., Uchiumi, T., Hayakawa, H., Ono, M., Wada, M., Izumi, H., and Kohno, K. (2003). The basic and clinical implications of ABC transporters, Y-box-binding protein-1 (YB-1) and angiogenesis-related factors in human malignancies. Cancer Sci. *94*, 9–14.

25. Wang, Y., Chen, Y., Geng, H., Qi, C., Liu, Y., and Yue, D. (2015). Overexpression of YB1 and EZH2 are associated with cancer metastasis and poor prognosis in renal cell carcinomas. Tumour Biol. *36*, 7159–7166.

26. Calise, S.J., Purich, D.L., Nguyen, T., Saleem, D.A., Krueger, C., Yin, J.D., and Chan, E.K. (2016). 'Rod and ring' formation from IMP dehydrogenase is regulated through the one-carbon metabolic pathway. J. Cell Sci. *129*, 3042–3052.

27. Jung, K., Wu, F., Wang, P., Ye, X., Abdulkarim, B.S., and Lai, R. (2014). YB-1 regulates Sox2 to coordinately sustain stemness and tumorigenic properties in a phenotypically distinct subset of breast cancer cells. BMC Cancer *14*, 328.

28. Wu, K., Chen, K., Wang, C., Jiao, X., Wang, L., Zhou, J., Wang, J., Li, Z., Addya, S., Sorensen, P.H., et al. (2014). Cell fate factor DACH1 represses YB-1-mediated oncogenic transcription and translation. Cancer Res. *74*, 829–839.

29. Chen, K., Zhang, J., Tastan, O.Y., Deussen, Z.A., Siswick, M.Y., and Liu, J.L. (2011). Glutamine analogs promote cytoophidium assembly in human and Drosophila cells. J. Genet. Genomics *38*, 391–402.

30. Chang, C.C., Lin, W.C., Pai, L.M., Lee, H.S., Wu, S.C., Ding, S.T., Liu, J.L., and Sung, L.Y. (2015). Cytoophidium assembly reflects upregulation of IMPDH activity. J. Cell Sci. *128*, 3550–3555.

31. Keppeke, G.D., Calise, S.J., Chan, E.K., and Andrade, L.E. (2015). Assembly of IMPDH2-based, CTPS-based, and mixed rod/ring structures is dependent on cell type and conditions of induction. J. Genet. Genomics *42*, 287–299.

32. Luo, C., Tetteh, P.W., Merz, P.R., Dickes, E., Abukiwan, A., Hotz-Wagenblatt, A., Holland-Cunz, S., Sinnberg, T., Schittek, B., Schadendorf, D., et al. (2013). miR-137 inhibits the invasion of melanoma cells through downregulation of multiple oncogenic target genes. J. Invest. Dermatol. *133*, 768–775.

33. Powles, T., Staehler, M., Ljungberg, B., Bensalah, K., Canfield, S.E., Dabestani, S., Giles, R.H., Hofmann, F., Hora, M., Kuczyk, M.A., et al. (2016). European Association of Urology Guidelines for Clear Cell Renal Cancers That Are Resistant to Vascular Endothelial Growth Factor Receptor-Targeted Therapy. Eur. Urol. *70*, 705–706.

34. Skinnider, B.F., Folpe, A.L., Hennigar, R.A., Lim, S.D., Cohen, C., Tamboli, P., Young, A., de Peralta-Venturina, M., and Amin, M.B. (2005). Distribution of cytokeratins and vimentin in adult renal neoplasms and normal renal tissue: potential utility of a cytokeratin antibody panel in the differential diagnosis of renal tumors. Am. J. Surg. Pathol. *29*, 747–754.

35. Avery, A.K., Beckstead, J., Renshaw, A.A., and Corless, C.L. (2000). Use of antibodies to RCC and CD10 in the differential diagnosis of renal neoplasms. Am. J. Surg. Pathol. *24*, 203–210.

36. Rocca, P.C., Brunelli, M., Gobbo, S., Eccher, A., Bragantini, E., Mina, M.M., Ficarra, V., Zattoni, F., Zamò, A., Pea, M., et al. (2007). Diagnostic utility of S100A1 expression in renal cell neoplasms: an immunohistochemical and quantitative RT-PCR study. Mod. Pathol. *20*, 722–728.

37. Memeo, L., Jhang, J., Assaad, A.M., McKiernan, J.M., Murty, V.V., Hibshoosh, H., Tong, G.X., and Mansukhani, M.M. (2007). Immunohistochemical analysis for cytokeratin 7, KIT, and PAX2: value in the differential diagnosis of chromophobe cell carcinoma. Am. J. Clin. Pathol. *127*, 225–229.

38. Gupta, R., Balzer, B., Picken, M., Osunkoya, A.O., Shet, T., Alsabeh, R., Luthringer, D., Paner, G.P., and Amin, M.B. (2009). Diagnostic implications of transcription factor Pax 2 protein and transmembrane enzyme complex carbonic anhydrase IX immunoreactivity in adult renal epithelial neoplasms. Am. J. Surg. Pathol. *33*, 241–247.

39. Tan, P.H., Cheng, L., Rioux-Leclercq, N., Merino, M.J., Netto, G., Reuter, V.E., Shen, S.S., Grignon, D.J., Montironi, R., Egevad, L., et al.; ISUP Renal Tumor Panel (2013). Renal tumors: diagnostic and prognostic biomarkers. Am. J. Surg. Pathol. *37*, 1518–1531.

40. Boysen, G., Bausch-Fluck, D., Thoma, C.R., Nowicka, A.M., Stiehl, D.P., Cima, I., Luu, V.D., von Teichman, A., Hermanns, T., Sulser, T., et al. (2012). Identification and functional characterization of pVHL-dependent cell surface proteins in renal cell carcinoma. Neoplasia *14*, 535–546.

41. Ruan, H., Li, X., Yang, H., Song, Z., Tong, J., Cao, Q., Wang, K., Xiao, W., Xiao, H., Chen, X., et al. (2017). Enhanced expression of caveolin-1 possesses diagnostic and prognostic value and promotes cell migration, invasion and sunitinib resistance in the clear cell renal cell carcinoma. Exp. Cell Res. *358*, 269–278.

42. Wang, T., Song, W., Chen, Y., Chen, R., Liu, Z., Wu, L., Li, M., Yang, J., Wang, L., Liu, J., et al. (2016). Flightless I Homolog Represses Prostate Cancer Progression through Targeting Androgen Receptor Signaling. Clin. Cancer Res. *22*, 1531–1544.

43. Nghiem, B., Zhang, X., Lam, H.M., True, L.D., Coleman, I., Higano, C.S., Nelson, P.S., Pritchard, C.C., and Morrissey, C. (2016). Mismatch repair enzyme expression in primary and castrate resistant prostate cancer. Asian J. Urol. *3*, 223–228.

44. Tao, Z., Ruan, H., Sun, L., Kuang, D., Song, Y., Wang, Q., Wang, T., Hao, Y., and Chen, K. (2019). Targeting the YB-1/PD-L1 Axis to Enhance Chemotherapy and Antitumor Immunity. Cancer Immunol. Res. *7*, 1135–1147.

45. Kaeser, M.D., and Iggo, R.D. (2002). Chromatin immunoprecipitation analysis fails to support the latency model for regulation of p53 DNA binding activity in vivo. Proc. Natl. Acad. Sci. USA *99*, 95–100.

46. Ruan, H., Yang, H., Wei, H., Xiao, W., Lou, N., Qiu, B., Xu, G., Song, Z., Xiao, H., Liu, L., et al. (2017). Overexpression of SOX4 promotes cell migration and invasion of renal cell carcinoma by inducing epithelial-mesenchymal transition. Int. J. Oncol. *51*, 336–346.

47. Chen, X., Wang, X., Ruan, A., Han, W., Zhao, Y., Lu, X., Xiao, P., Shi, H., Wang, R., Chen, L., et al. (2014). miR-141 is a key regulator of renal cell carcinoma proliferation and metastasis by controlling EphA2 expression. Clin. Cancer Res. *20*, 2617–2630.

48. Xu, S., Tao, Z., Hai, B., Liang, H., Shi, Y., Wang, T., Song, W., Chen, Y., OuYang, J., Chen, J., et al. (2016). miR-424(322) reverses chemoresistance via T-cell immune response activation by blocking the PD-L1 immune checkpoint. Nat. Commun. *7*, 11406.